Separation of the σ_L and σ_T contributions to the production of hadrons in electroproduction

H. Avakian, T. B. Hayward, K. Joo, U. Shrestha et al.
For the CLAS Collaboration

PAC 51
July 24, 2023

UCONN | UNIVERSITY OF CONNECTICUT

clas

Motivation

- **This proposal aims to perform the first multidimensional, high statistics Rosenbluth separation of the L- and T- polarized virtual photon contributions to the SIDIS cross section using the RGA 10.6 GeV, RGK 6.5 and 7.5 GeV, and the proposed RGK 8.4 GeV measurements**.

- The main motivation is to test that the TMD factorization is based on γ_T dominance.

- Recent measurements at HERMES, COMPASS, JLab, etc. have assumed that $R_{SIDIS} = R_{DIS}$ which can introduce significant uncertainties when using SIDIS data to infer quark flavor and spin distributions (e.g. at large non perturbative P_T; which just so happens to be the region with the largest difficulty in reconciling phenomenological attempts to describe the data).

- R_{SIDIS} measurement is critical for all previous, current and future SIDIS measurements, including EIC and JLab 22 GeV.

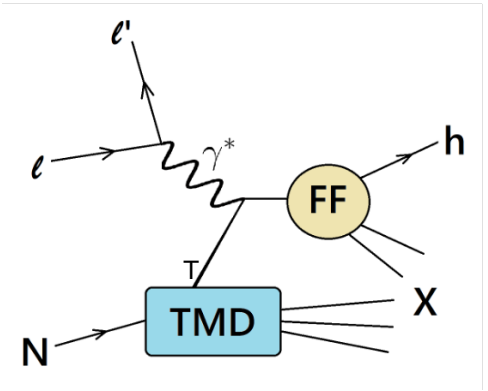

γ^*_T dominance

Previous study for $R = \sigma_L/\sigma_T$ in SIDIS

$$\frac{d\sigma}{dxdQ^2dzdP_T^2d\phi} = \frac{\pi\alpha^2}{x^2Q^4}\frac{(2x+\gamma^2)}{(1+\gamma^2)}K(y)\left(F_{UU,T} + \epsilon F_{UU,L} + \sqrt{2\epsilon(1+\epsilon)}\cos\phi F_{UU}^{\cos\phi} + \epsilon\cos(2\phi)F_{UU}^{\cos(2\phi)}\right)$$

$$K(y) = 1 - y + y^2/2 + \gamma^2y^2/4, \qquad \varepsilon = \frac{1 - y - \frac{1}{4}\gamma^2y^2}{1 - y + \frac{1}{2}y^2 + \frac{1}{4}\gamma^2y^2}$$

- The contributions of $F_{UU,L}$ should not be ignored when $F_{UU,T}$ is extracted.
- Brief study at Cornell synchrotron in the 70s (moderate Q^2 and W, small ε separation, integrated over a very low P_T).

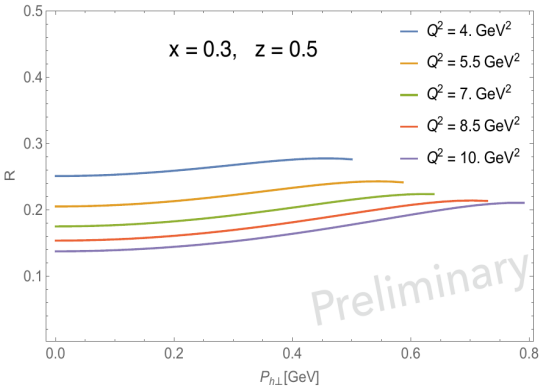

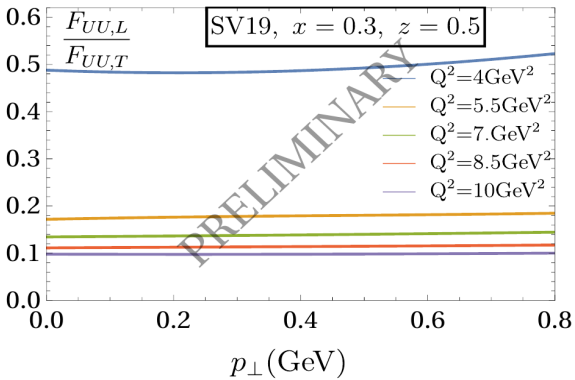

Estimate of $R_{\rm SIDIS} = F_{UU,L}/F_{UU,T}$ at fixed values of x and z and for different values of Q^2 using MAP22 (left) and a simplified model (only u-quark) using SV19 (right).

MAP22 TMD, JHEP, 10:127, 2022. doi:10.1007/JHEP10(2022)127

Indications of increased L contribution at high P_T

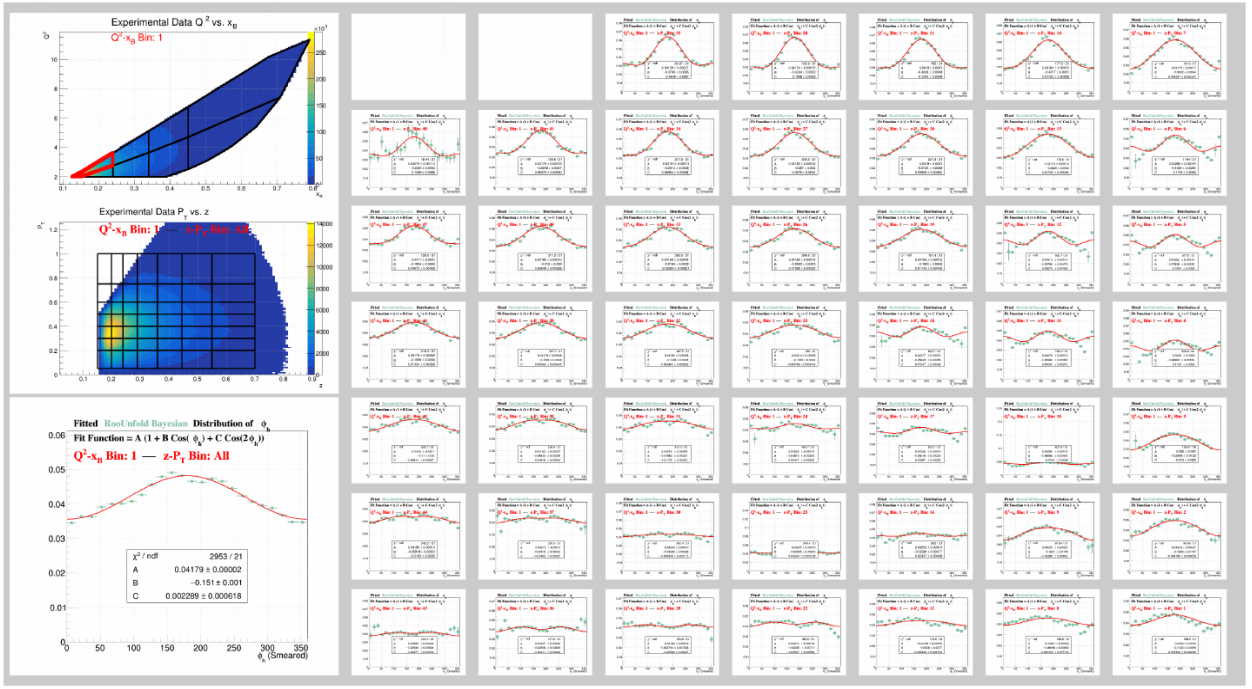

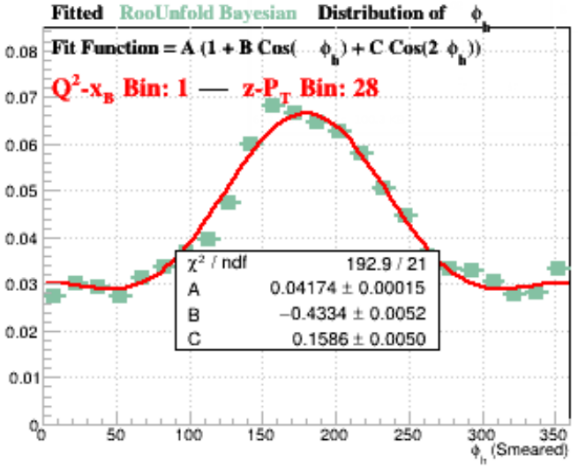

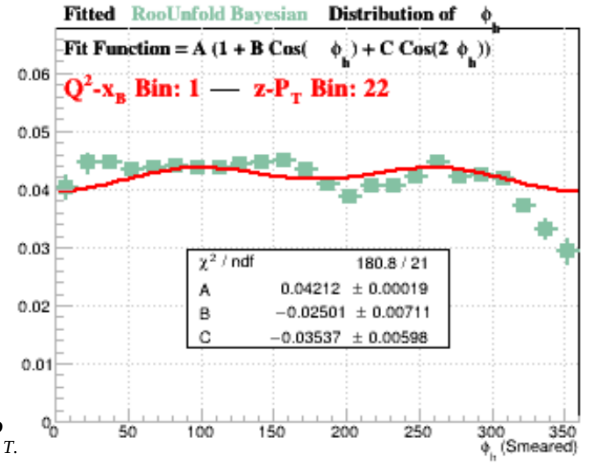

- At higher P_T , higher relative contributions of the *cosφ* amplitude than the *cos2φ*, indicates significant longitudinal photons contributions to the cross section.
- At large P_T both azimuthal modulations increase, making proper separation of azimuthal modulations important for precision measuremnts of the φ-independent structure functions, such as $F_{UU,T}$ and $F_{UU,L}$.
- We aim to study their P_T dependence, where the RGA data already implies a changing R_{SIDIS} value with P_T.

Rosenbluth Separation

Data & MC: RG-K eπ⁺

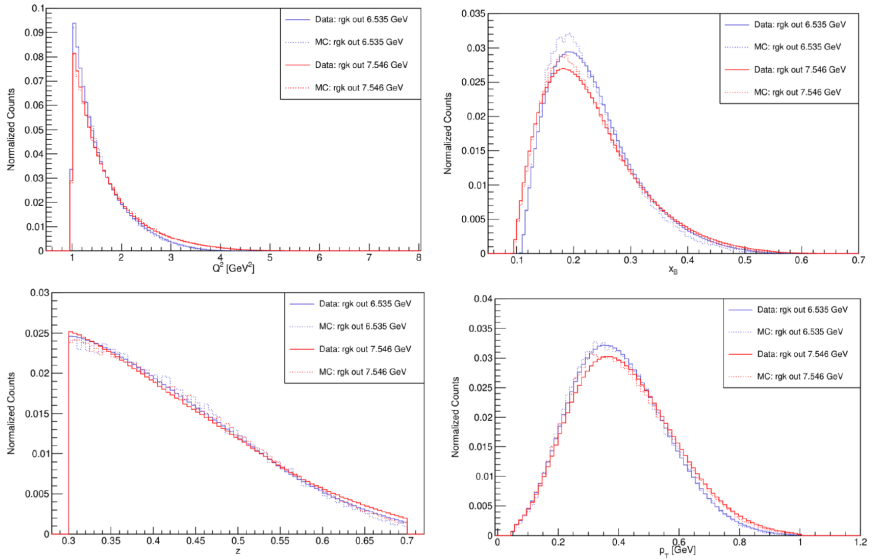

Channel Selection Cuts:

- $Q^2 > 1.00$ GeV^2, to select DIS events.
- $W > 2.00$ GeV, to avoid the resonance region.
- $y < 0.75$, to avoid the region most susceptible to radiative effects.
- $M_x > 1.50$ GeV, to avoid contributions from exclusive production.
- $x_F > 0$, to limit contributions from traget fragmentation
- $0.3 < z < 0.7$, to avoid target fragmentation and exclusive channels while focussing on the SIDIS region.

- Vary ε by keeping Q^2 and x fixed. This can be done by varying the beam energy.
- Three beam energies will be used, 6.535, 7.546, and 8.4 GeV from the RG-K outbending run and 10.6 GeV from the RG-A outbending run.
- For a particular x-Q^2 bin, and for integrated z, P_T and φ, the cross sections can be expressed as,

$$\frac{d\sigma}{dxdQ^2dzdP_T} = GK(y)\left(F_{UU,T} + \epsilon F_{UU,L}\right)$$

- A straight line fit is performed to the extract $F_{UU,T}$ and $F_{UU,L}$ for different points at each fixed Q^2 and x point.
- The intercept yields $F_{UU,T}$ and the slope gives $F_{UU,L}$.
- The procedure was tested with MC data sets for 6.535, 7.546, 8.4 and 10.6 GeV beam energies. With observed resolutions in the kinematic variables, the choice of a 0.02 step in x and 0.2 in Q^2 was tested.
- Sample Bin: $0.3 < x < 0.32$, $2.4 < Q^2 < 2.6$, $0.2 < z < 0.7$, $0.3 < P_T < 0.6$
- R measurements are made using MC for $e\pi^+$, $e\pi$, and dihadron channels.

Kinematic Distributions

$0.3 < x < 0.32$, $2.4 < Q^2 < 2.6$, $0.2 < z < 0.7$, $0.3 < P_T < 0.6$

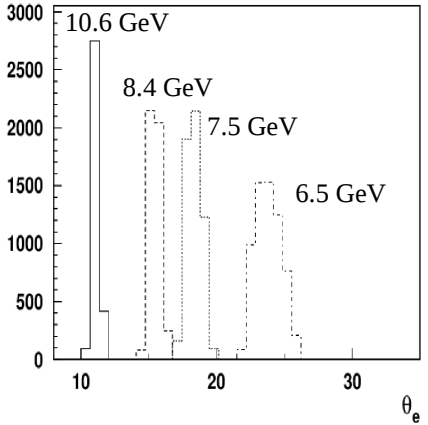

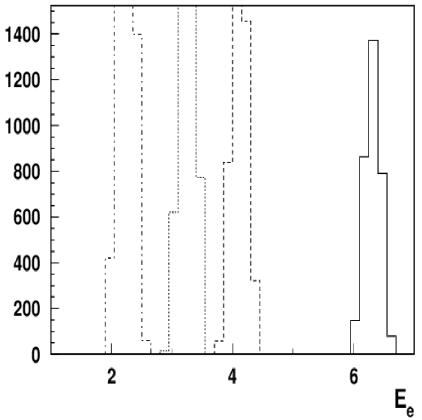

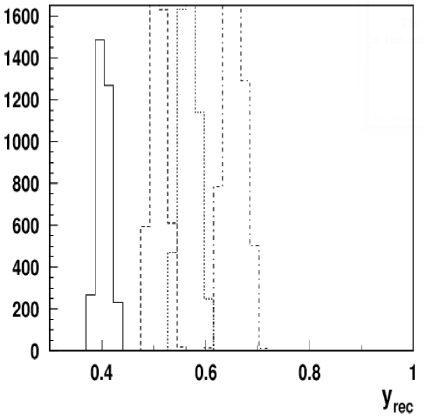

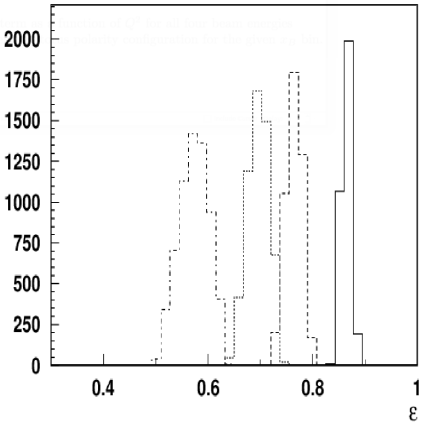

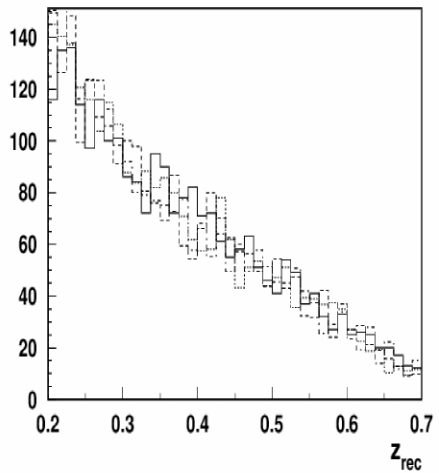

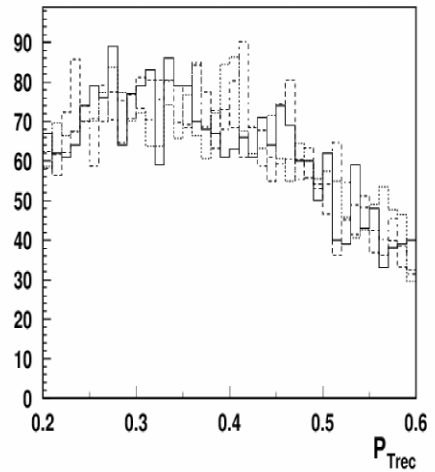

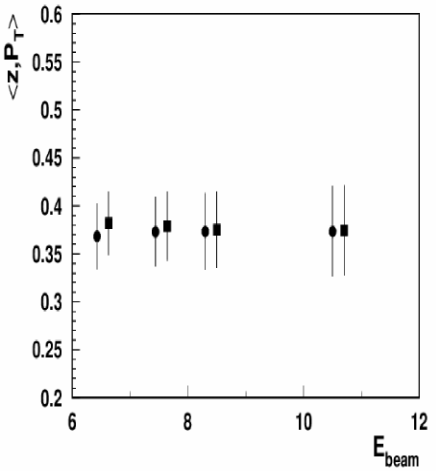

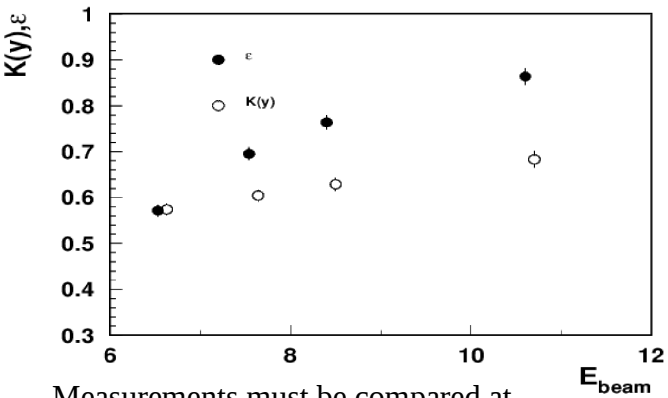

Measurements must be compared at fixed Q^2 and x but varying ε

Extraction of *R* (from MC)

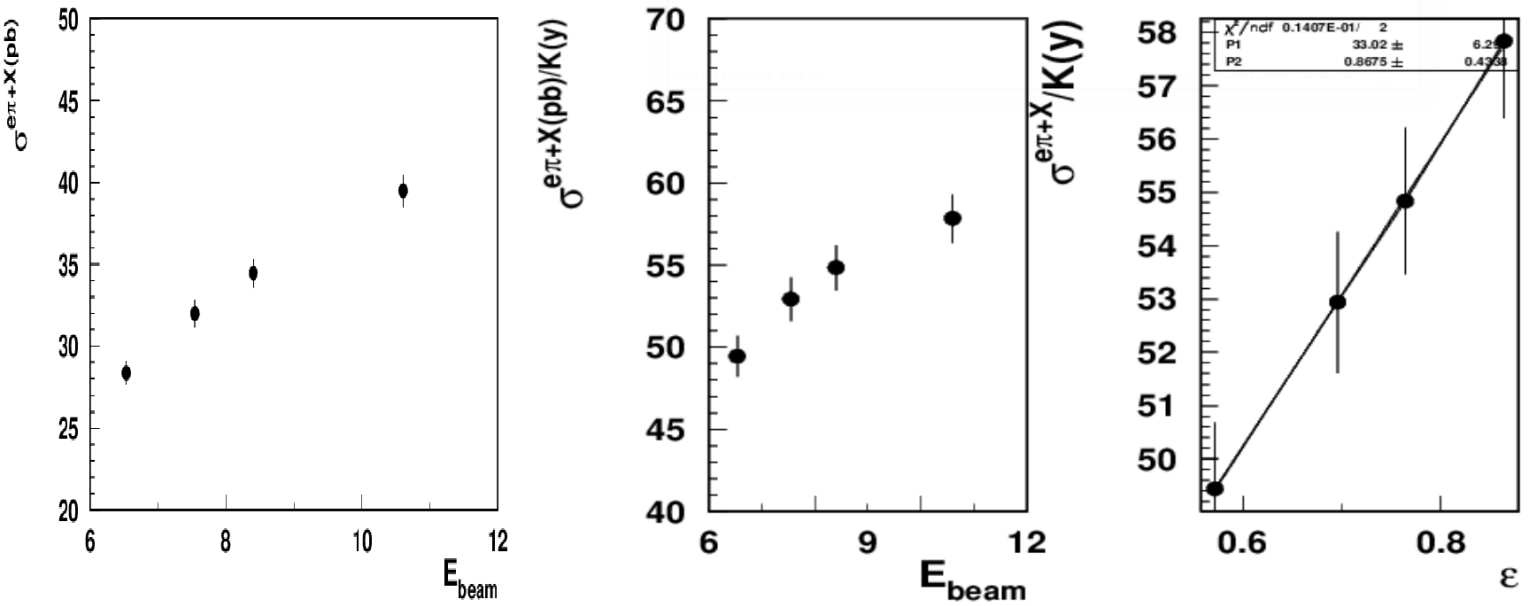

The integrated cross section for $ep \to e'\pi^+X$ in the given bin as a function of the beam energy (left).
The same cross section scaled by the energy-dependent kinematic factor K(y) (middle) for a single bin.
The normalized by the kinematic factor cross sections fitted with a linear function $P_1(1+\epsilon P_2)$, with $R = P_2$ (right).

Extraction of R (dihadron sample)

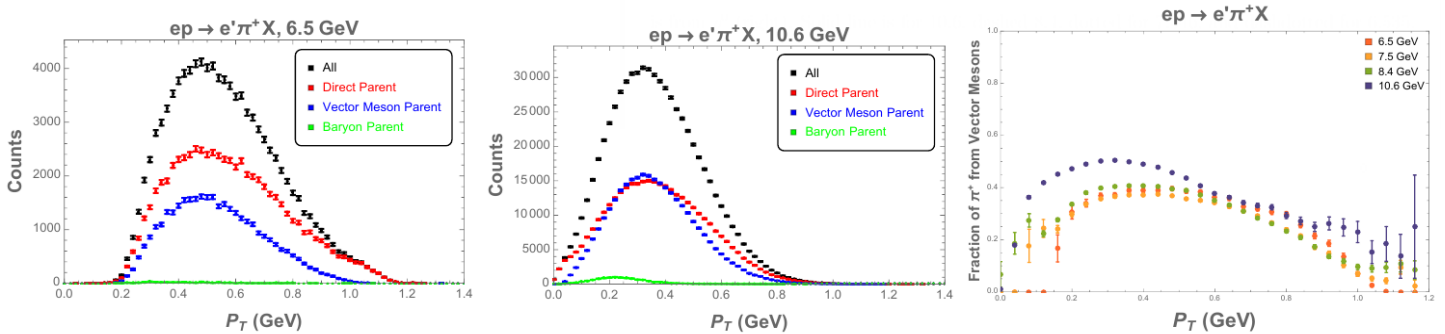

The P_T distribution for all π^+ (black), π^+ directly produced from the struck quark (red), π^+ from a vector meson parent (blue) and π^+ from a baryon parent (green) for 6.5 GeV (left) and 10.6 GeV (middle) and the fraction of π^+ coming from a vector meson parent as a function of P_T for all four beam energies (right).

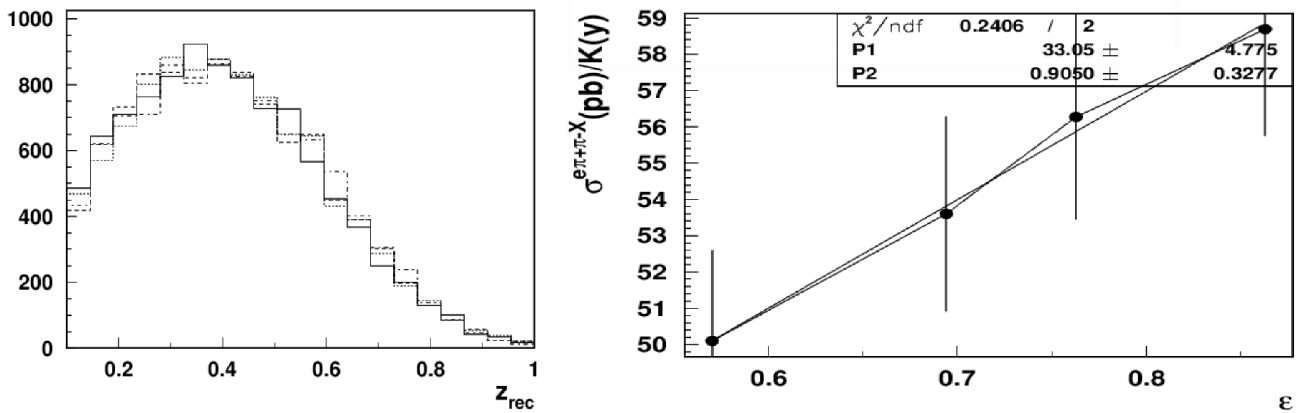

The z-dependence for different energies (left) and extracted R for the dihadron sample integrated over z and M_h

Systematic Uncertainties

- Different sources of systematic uncertainty were found to be small.
- Kaon contamination in the pion sample is ~ 1 - 2% (with cut on $p < 5$ GeV and additional cut on χ^2 value).
- Baryon resonance contamination is at a few percent level (with cut on $M_x > 1.5$ GeV).
- Charge symmetric background contamination is less than 1% (with cut on $y < 0.75$).
- Radiative Corrections at large P_T can be significant, but within the phase space used, the relative corrections remain below 5% (large P_T for lower Q^2 is cut by $M_x > 1.5$ GeV and lower energies for higher Q^2 is cut by $y < 0.75$).
- For our concerned kinematic range, the variation of the reconstruction efficiency between low- and high-luminosity run demonstrated very little kinematic dependence.
- Similarly, the contributions from the sector dependence is expected to be smaller.
- We aim for the total systematic uncertainty to be below 5%.

Summary

- SIDIS measurements have relied on the assumption that $R_{SIDIS} = R_{DIS}$, thereby introducing considerable uncertainties when using SIDIS data to deduce the flavor and spin distributions of the quarks.
- We propose an add-on experiment to the RG-K run group, aimed to provide an in-depth analysis of the SIDIS cross sections for single and dihadron production.
- Combining the RG-A and RG-K runs, L/T separation will be performed in a wide range of kinematics of Q^2, x_B, P_T, and z.
- For higher Q^2 the new RG-K measurements with 8.4 GeV beam will be critical.
- Our results will extend in phase space combining high-precision future measurements planned at Hall-C with wide acceptance measurments with CLAS12.
- Direct measurement of R_{SIDIS} will allow more precise determinations of quark distributions and their interactions within the nucleon, providing critical input for the evaluation of systematics in phenomenological studies.

Thank you!

Extras

Longitudinal photon contributions in SIDIS

A. Bacchetta

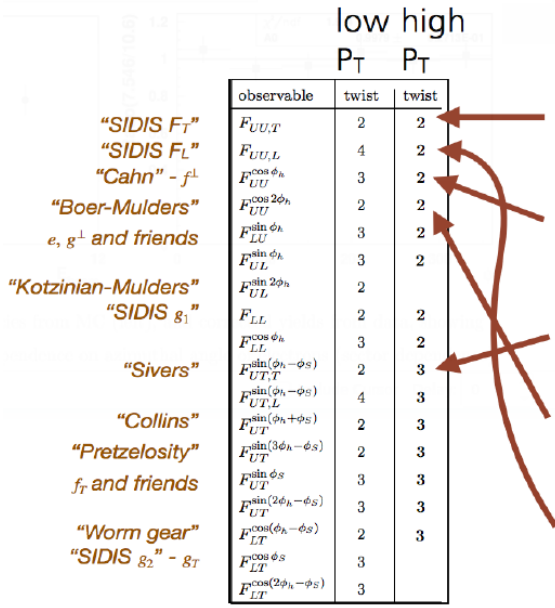

There are several possibilities:

- Twist 2 TMD matching twist 2 PDF
- Twist 3 TMD matching twist 2 PDF
- Twist 2 TMD matching twist 3 PDF
- Expected mismatch
- Twist 4 TMD matching twist 2 PDF?

→ Contributes everywhere,
→ we know nothing!!!

$$\frac{d\sigma}{dx\,dy\,dz\,dP_{h\perp}^2} = \frac{2\pi\alpha^2}{x\,y\,Q^2}\,\frac{y^2}{2\,(1-\varepsilon)}\left\{2\pi F_{UU,T}(x,z,P_{h\perp}^2,Q^2) + \varepsilon\,2\pi F_{UU,L}(x,z,P_{h\perp}^2,Q^2)\right\}$$

$$\frac{d\sigma}{dx\,dy\,dz} = \frac{4\pi\alpha^2}{x\,y\,Q^2}\,\frac{y^2}{2\,(1-\varepsilon)}\left\{F_{UU,T}(x,z,Q^2) + \varepsilon\,F_{UU,L}(x,z,Q^2)\right\}$$

$$R = \frac{F_{UU,L}}{F_{UU,T}}$$

Structure functions in SIDIS

- At large x fixed target experiments are sensitive to ALL Structure Functions
- At higher energies (EIC), observables surviving the $\varepsilon \to 1$ limit (F_{UU}, F_{UL}, Transversely pol. F_{UT})

$$\frac{d\sigma}{dx\,dy\,d\phi_S\,dz\,d\phi_h\,dP_h^2} = \frac{\alpha^2}{x\,y\,Q^2}\frac{y^2}{2\,(1-\varepsilon)}\Big\{ F_{UU,T} + \varepsilon F_{UU,L} + \sqrt{2\varepsilon(1+\varepsilon)}\cos\phi_h F_{UU}^{\cos\phi_h} + \varepsilon\cos(2\phi_h) F_{UU}^{\cos 2\phi_h}$$
$$+ \lambda_e \sqrt{2\varepsilon(1-\varepsilon)}\sin\phi_h F_{LU}^{\sin\phi_h} + S_L\left[\sqrt{2\varepsilon(1+\varepsilon)}\sin\phi_h F_{UL}^{\sin\phi_h} + \varepsilon\sin(2\phi_h) F_{UL}^{\sin 2\phi_h}\right]$$
$$+ S_L\,\lambda_e\left[\sqrt{1-\varepsilon^2}\,F_{LL} + \sqrt{2\varepsilon(1-\varepsilon)}\cos\phi_h F_{LL}^{\cos\phi_h}\right]$$
$$+ S_T\Big[\sin(\phi_h-\phi_S)\left(F_{UT,T}^{\sin(\phi_h-\phi_S)} + \varepsilon F_{UT,L}^{\sin(\phi_h-\phi_S)}\right) + \varepsilon\sin(\phi_h+\phi_S) F_{UT}^{\sin(\phi_h+\phi_S)}$$
$$+ \varepsilon\sin(3\phi_h-\phi_S) F_{UT}^{\sin(3\phi_h-\phi_S)} + \sqrt{2\varepsilon(1+\varepsilon)}\sin\phi_S F_{UT}^{\sin\phi_S}$$
$$+ \sqrt{2\varepsilon(1+\varepsilon)}\sin(2\phi_h-\phi_S) F_{UT}^{\sin(2\phi_h-\phi_S)}\Big] + S_T\lambda_e\Big[\sqrt{1-\varepsilon^2}\cos(\phi_h-\phi_S) F_{LT}^{\cos(\phi_h-\phi_S)}$$
$$+ \sqrt{2\varepsilon(1-\varepsilon)}\cos\phi_S F_{LT}^{\cos\phi_S} + \sqrt{2\varepsilon(1-\varepsilon)}\cos(2\phi_h-\phi_S) F_{LT}^{\cos(2\phi_h-\phi_S)}\Big]\Big\}$$

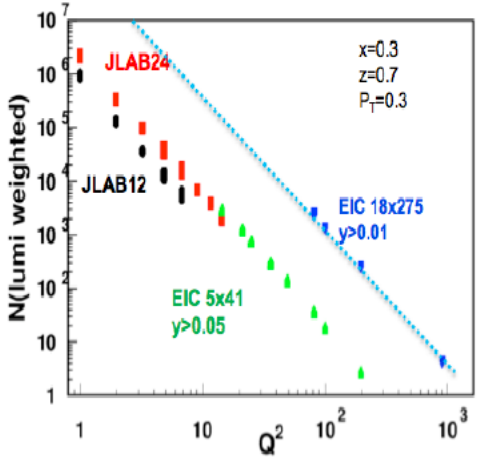

x-section from Bacchetta et al, 1703.10157

Combination of statistics and depolarization factors defines measurable SFs

Higher energy experiments so far were focused on

- $F_{UU,T}$ (Multiplicity/x-section)
- Sivers ($F_{UU,T}^{\sin(\phi-\phi S)}$)
- Collins ($F_{UT}^{\sin(\phi+\phi S)}$)

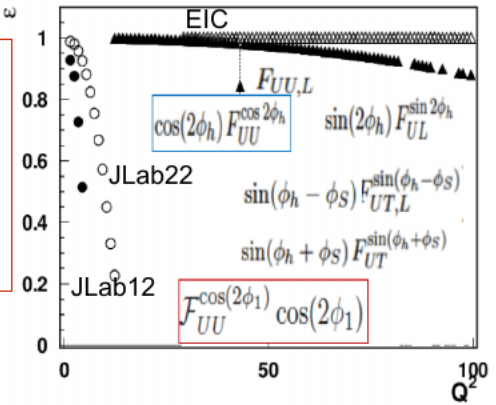

$R = \sigma_L/\sigma_T$ in resonace region and DIS

- Hall C data allows for Rosenbluth separation of 167 data points.
- First separate values of F_1 and F_L in this kinematic regime.

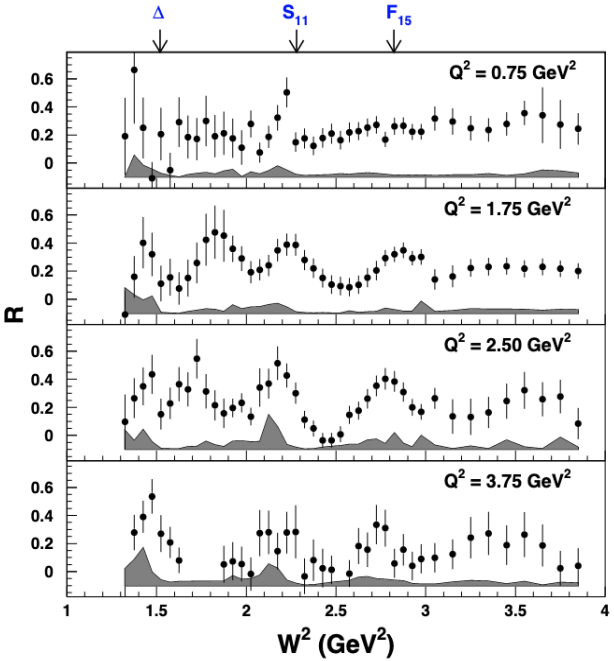

Y. Liang et al. (Jefferson Lab E94-110 Collaboration), [nucl-ex 0410027]

$$R \equiv \frac{\sigma_L}{\sigma_T} \equiv \frac{F_L}{2xF_1} = \frac{F_2}{2xF_1}\left(1 + \frac{4M^2x^2}{Q^2}\right) - 1$$

A. N. Hiller Blin et al., *Phys. Rev. C* 104 (2021) 2, 025201, [hep-ph 2105.05834]

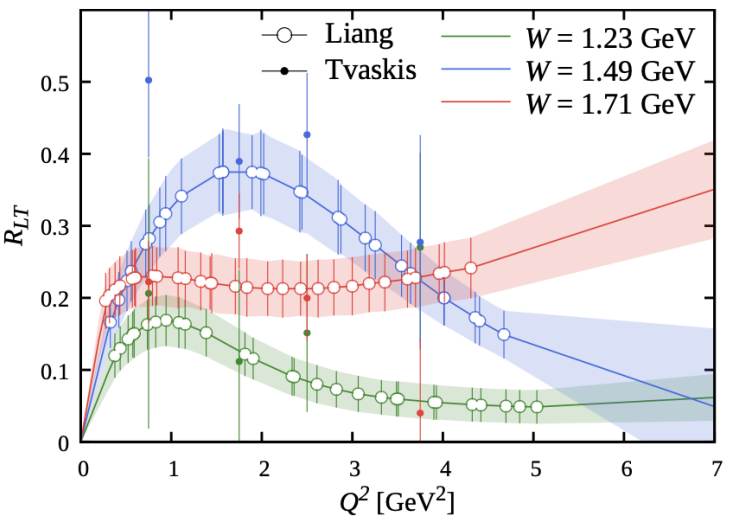

Predictions at higher Q^2 performed by fitting a second-degree polynomial to the grid of the Hall-C results.

FUU, Studies at Hall C

Ed Kinney

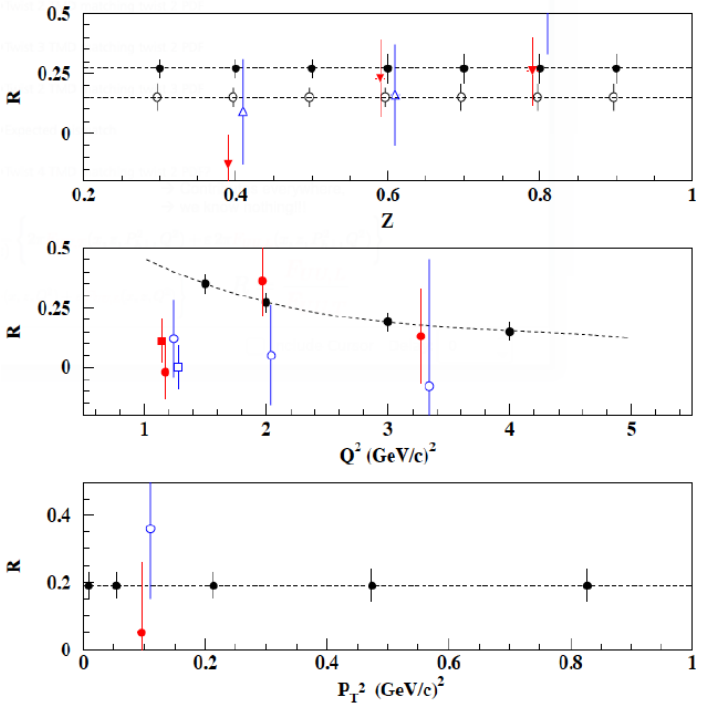

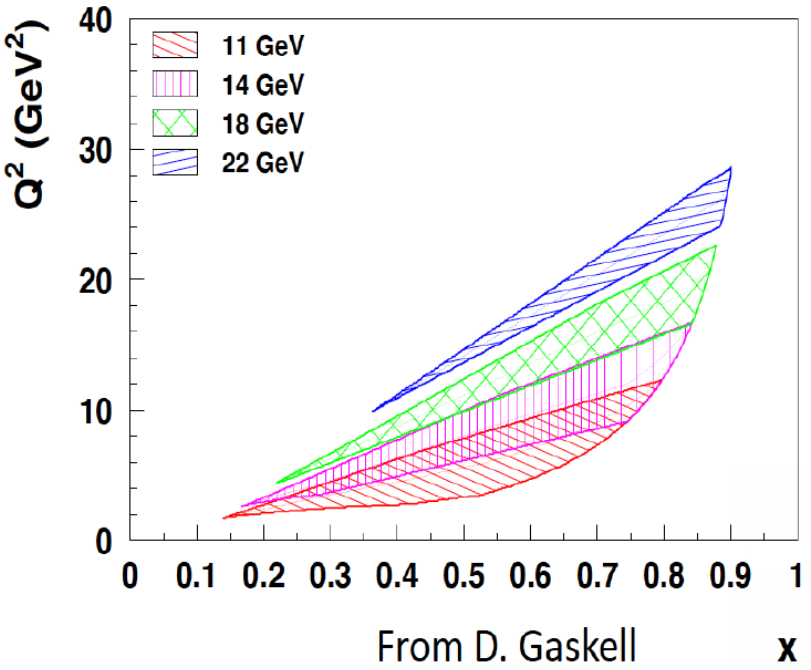

Projections for E12-06-104 vs existing Cornell Data (assume RSIDIS = RDIS)

Kinematic ranges accessible in Hall C with existing HMS and SHMS spectrometers and that can achieve two ε values separated by 0.2 with a minimum ε of 0.1

Data vs. MC comparison : RG-K eπ$^+$

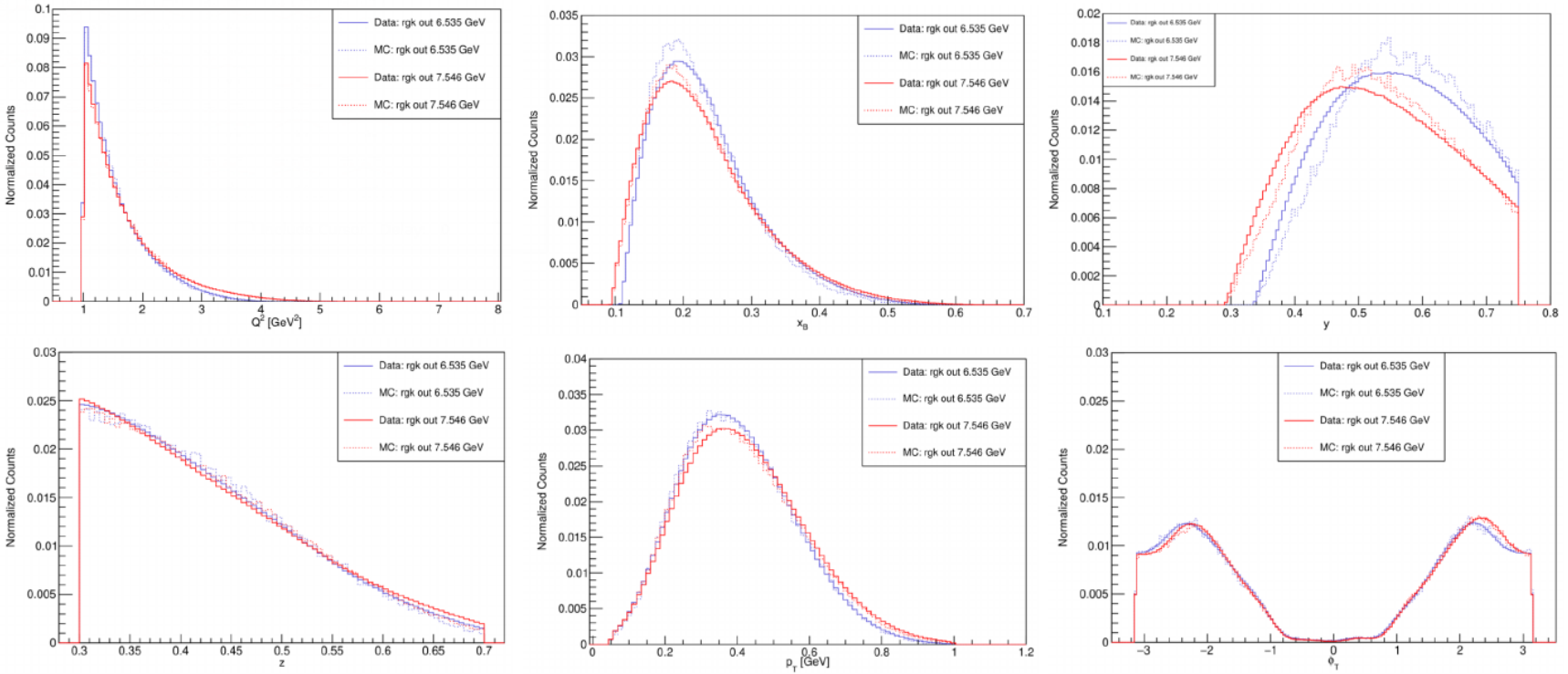

Comparisons between the clasdis MC (dotted lines) and collected CLAS12 data (solid lines) for 6.5 GeV (blue) and 7.5 GeV (red). The top row shows relevant DIS variables (Q^2, x and y) and the bottom row shows relevant SIDIS variables (z, P_T and ϕ). The data sets have been normalized to the total number of π^+.

Data vs. MC comparison : RG-A eπ$^+$

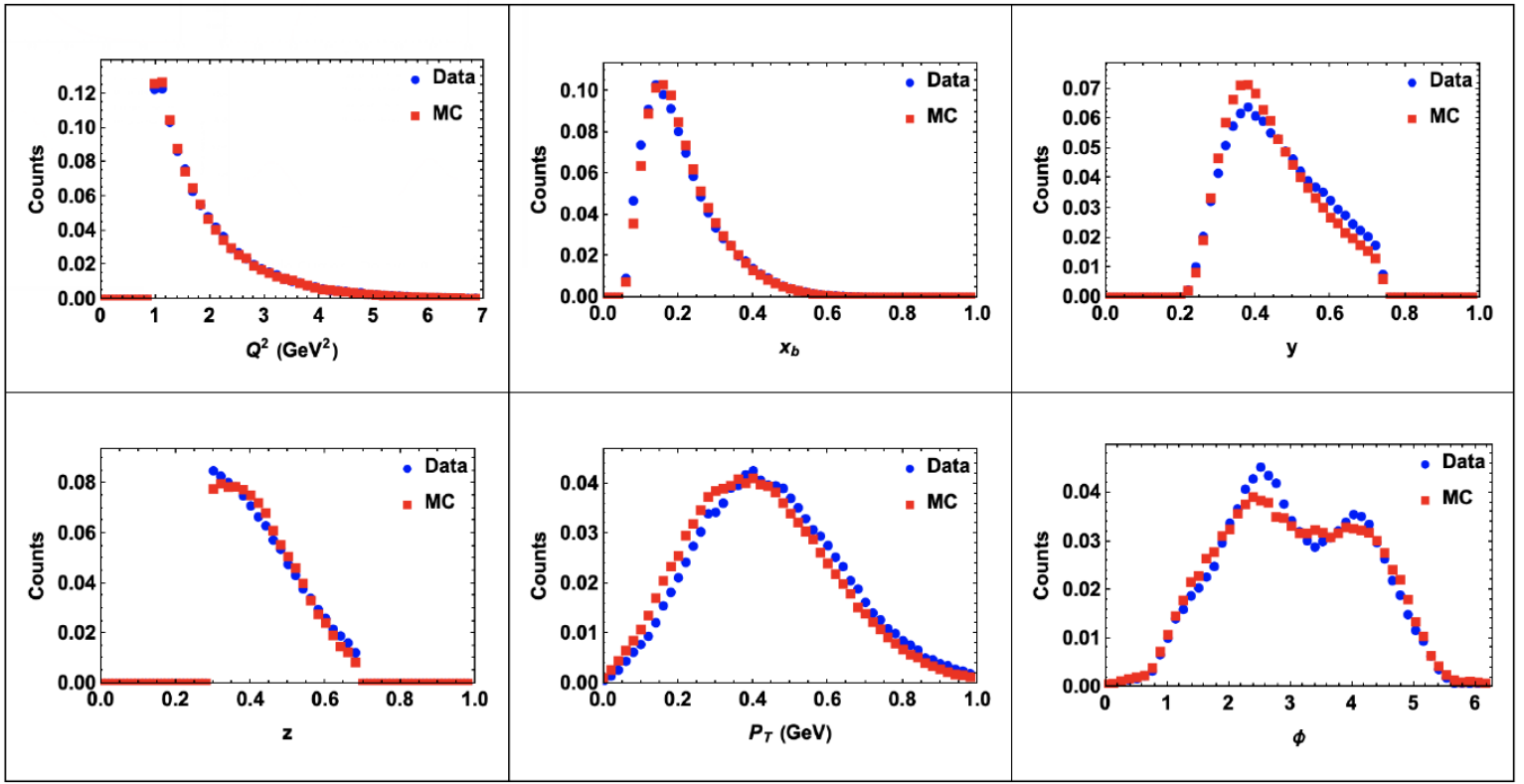

Comparisons between the integrated outbending 10.6 GeV clasdis MC (red) and RGA Fall18 outbending 10.6 GeV data (blue) samples for Q^2, x, y, z, P_T and ϕ. The datasets have been normalized to the total number of π^+.

Data vs. MC comparison : RG-A

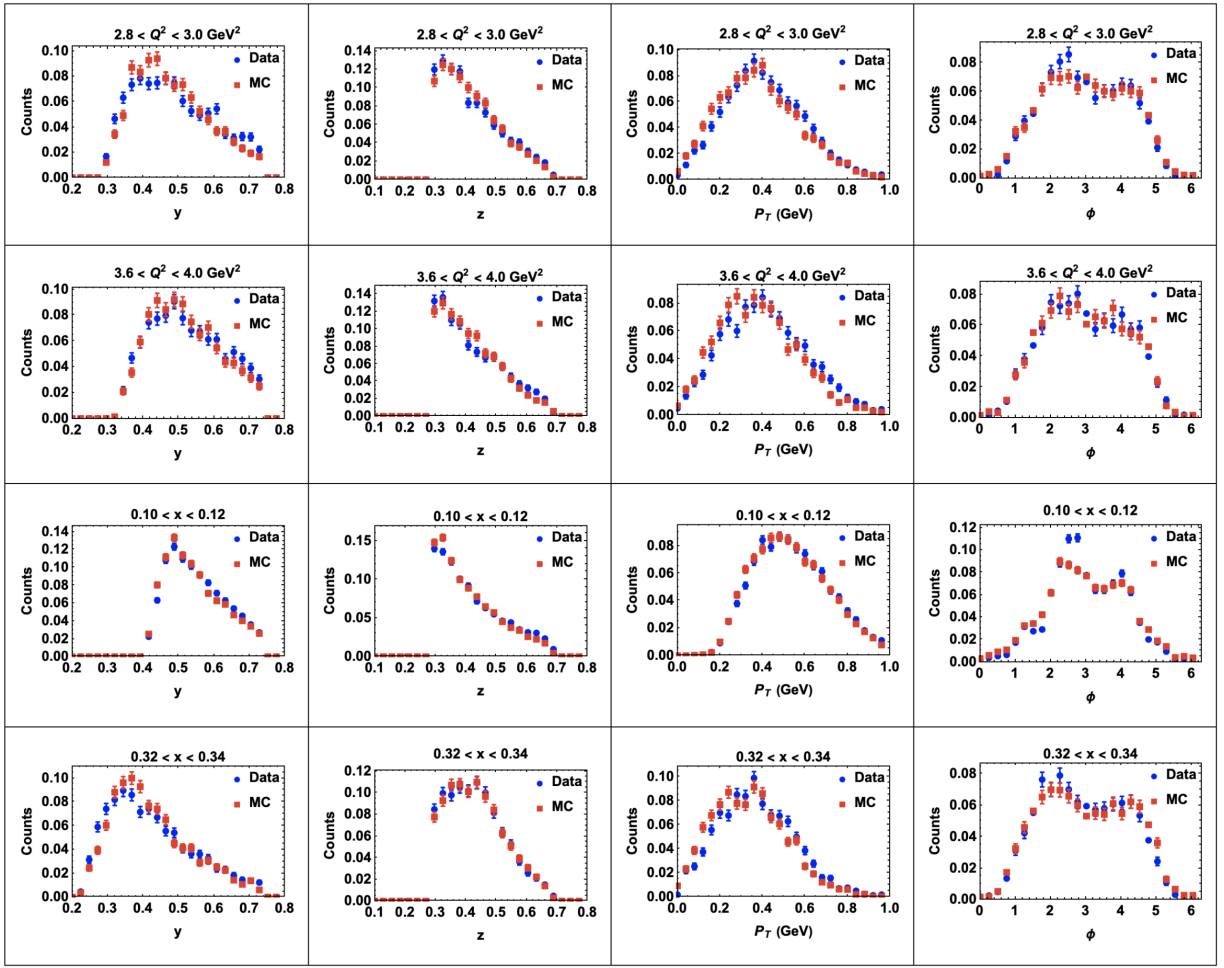

Scattered electrons and final state π^+ distributions

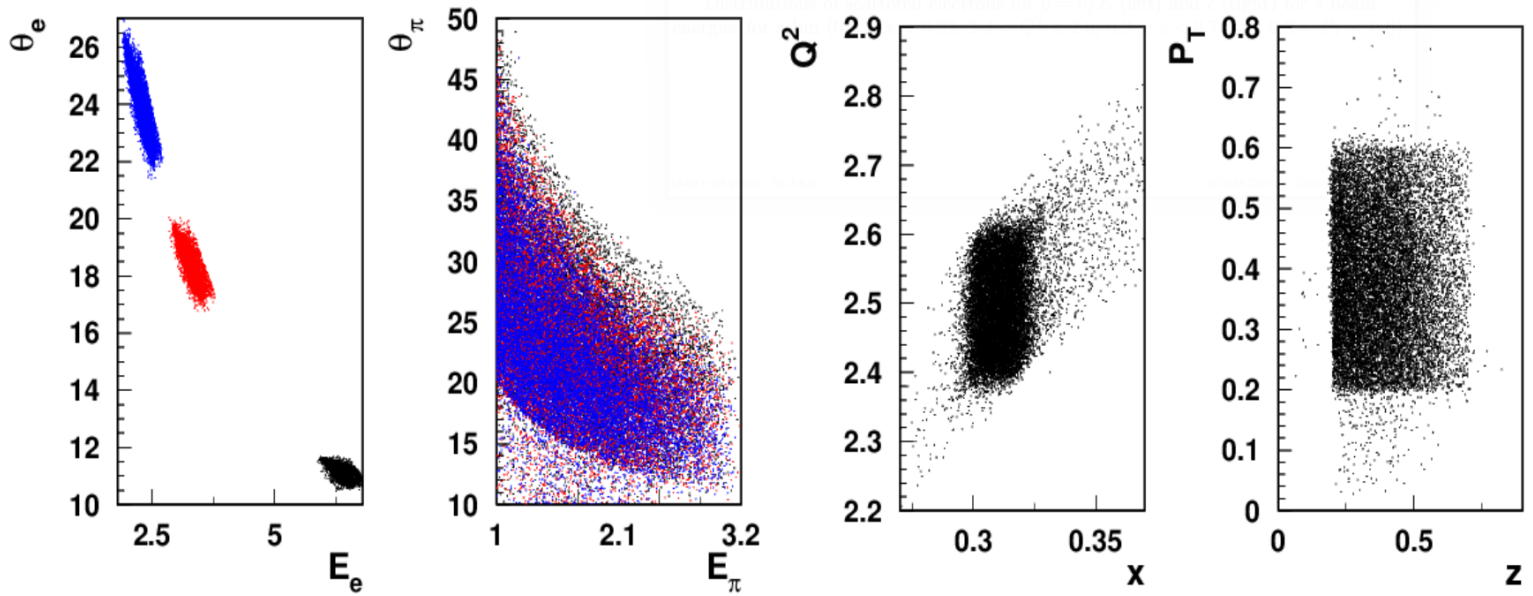

Distributions of scattered electrons and final state π^+ in momenta and angles (left), and in x vs Q^2 and pion z vs P_T (right) and momenta (right) for 3 beam energies for a bin ($0.3 < x < 0.32$, $2.4 < Q^2 < 2.6$, $0.2 < z < 0.7$, and $0.2 < P_T < 0.6$). The black dots are for 10.6 GeV, red for 7.5 GeV, and blue for 6.535 GeV.

Relevant kinematics are well separated

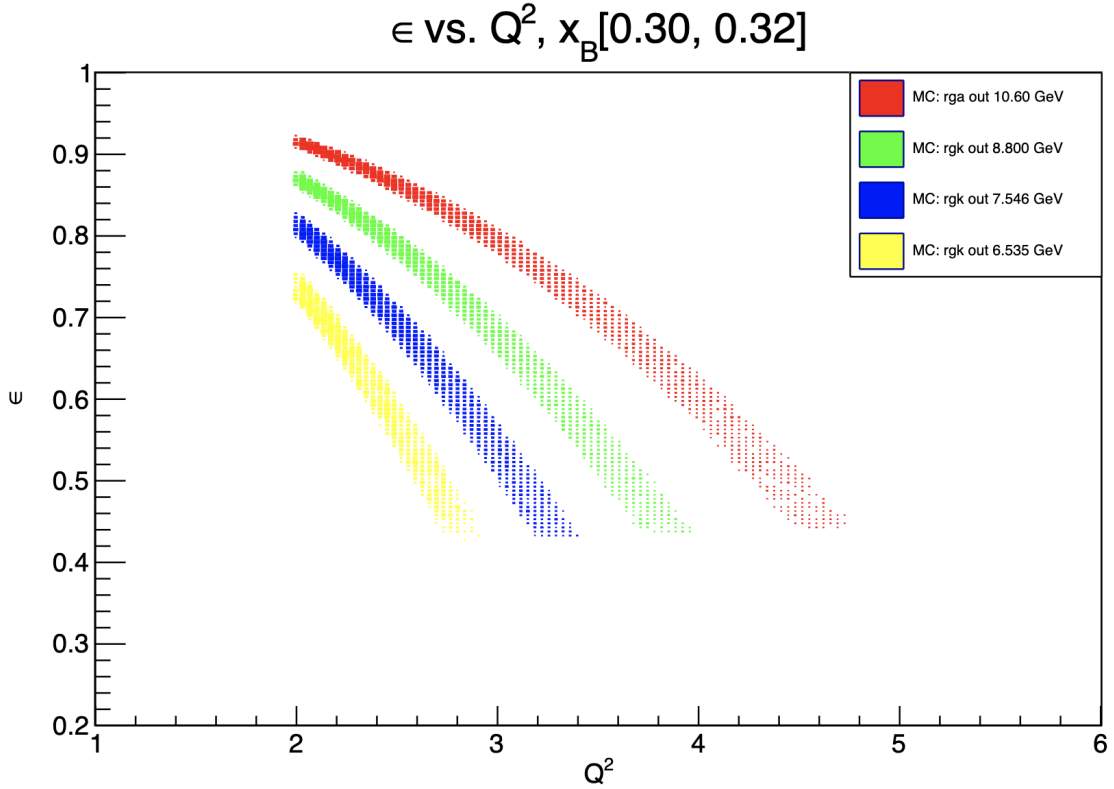

The ϵ-term as a function of Q^2 for all four beam energies in the outbending torus polarity configuration for the given x_B bin.

Extraction of *R* (from MC)

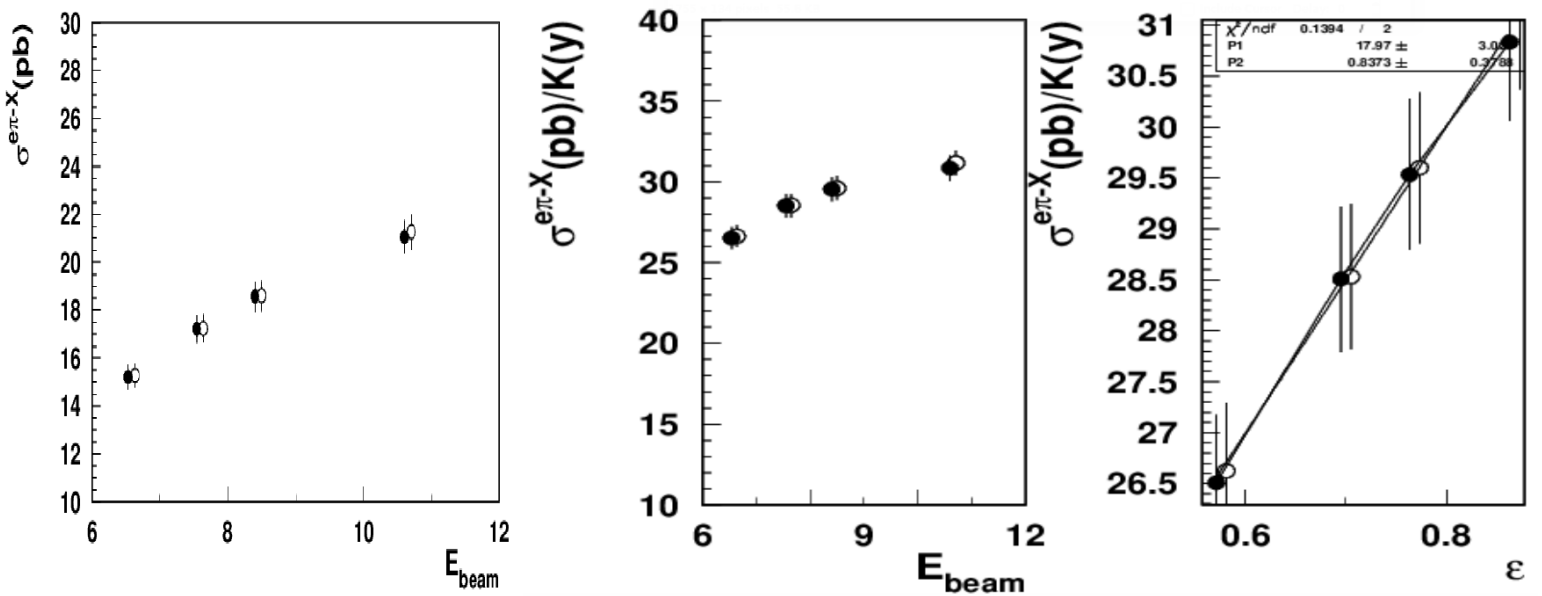

The integrated cross section for $ep \to e'\pi^- X$ in the given bin as a function of the beam energy (left).
The same cross section scaled by the energy-dependent kinematic factor K(y) (middle) for a single bin.
The normalized by the kinematic factor cross sections fitted with a linear function $P_1(1 + \epsilon P_2)$, with $R = P_2$ (right).

Extraction of *R* (from MC)

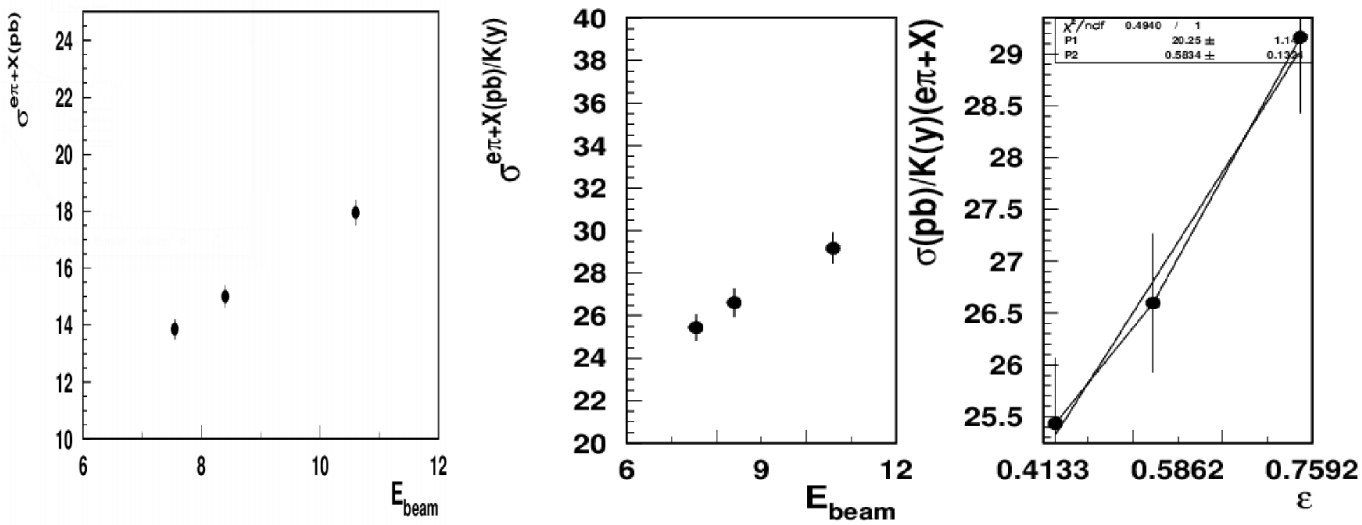

FIG. 19: The integrated cross section in a given bin as a function of the beam energy (left), the same cross section scaled by the energy-dependent kinematic factor K(y) (middle) for a higher Q^2 bin $3.2 < Q^2 < 3.4$. The normalized by the kinematic factor cross sections for $ep \to e'\pi^+X$, was fitted with a linear function $P_1(1 + \epsilon P_2)$, with $R = P_2$ (right). The value of R is 0.6 for the average Q^2 of 3.3 GeV^2.

Extraction of *R* (from MC)

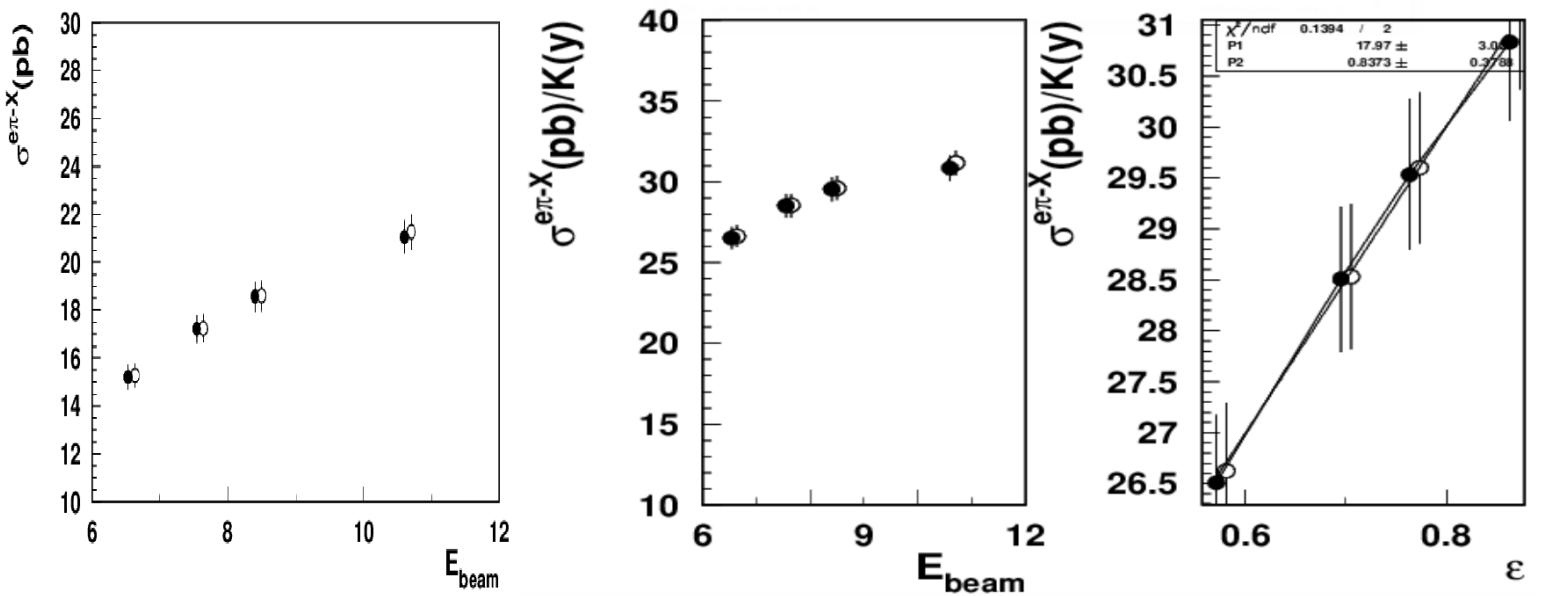

The integrated cross section for $ep \to e'\pi^- X$ in the given bin as a function of the beam energy (left).
The same cross section scaled by the energy-dependent kinematic factor K(y) (middle) for a single bin.
The normalized by the kinematic factor cross sections fitted with a linear function $P_1(1 + \epsilon P_2)$, with $R = P_2$ (right).

Extraction of *R* (dihadron sample)

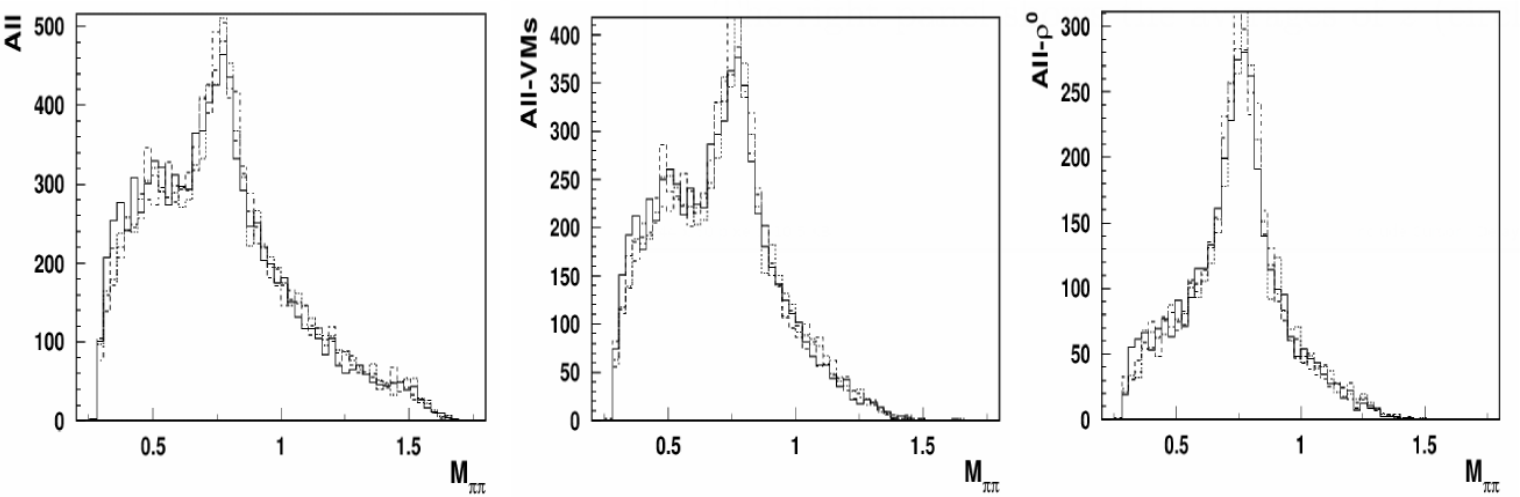

Distributions of $\pi^+\pi^-$ events as a function of their invariant mass, M_h, for the total sample (left) the sample with one of the pions from a VM decay (middle) and when one of the pions is from ρ^0 (right). Solid line is for 10.6, dashed 8.4, dotted for 7.546, and dashdotted for 6.535.

Systematic Uncertainties

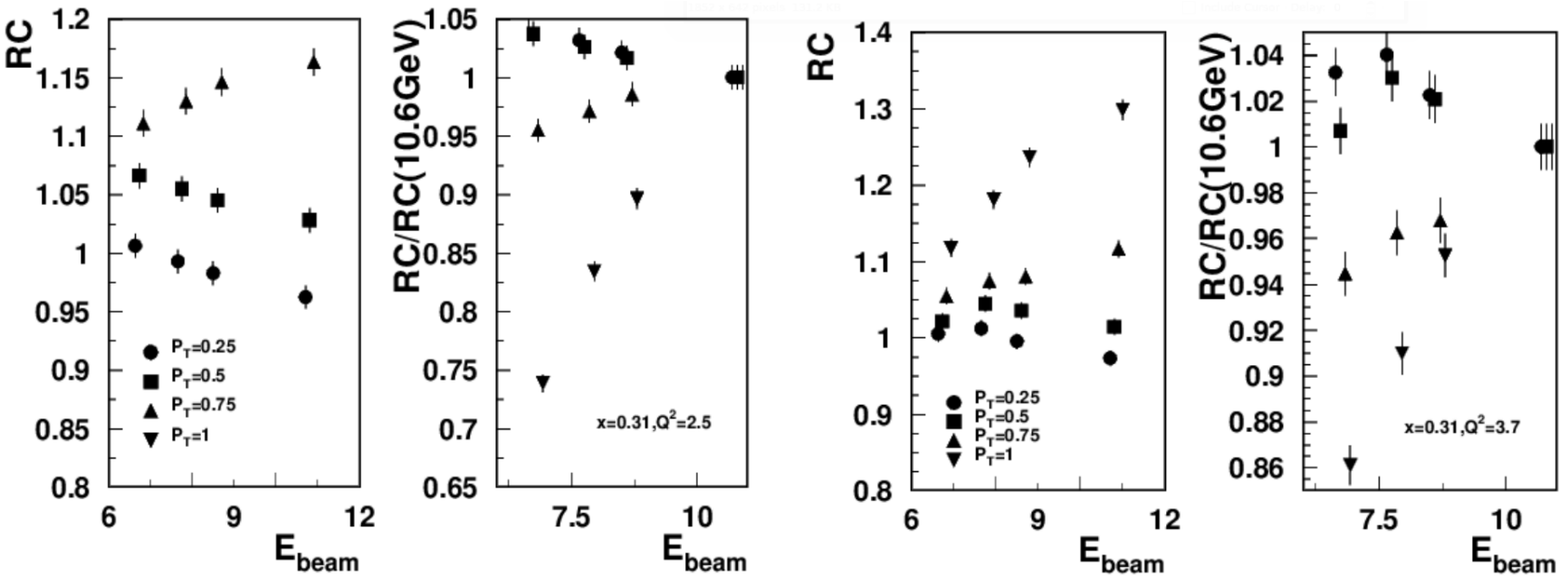

Radiative corrections (RC=σ_R/σ_B) to SIDIS cross section (left panel) and RC relative to values at 10.6 GeV (right panel) for two bins with $Q^2 = 2.5$ (left) and $Q^2 = 3.7$ (right) for the same $x = 0.31$ bin calculated at $z = 0.4$.

Systematic Uncertainties

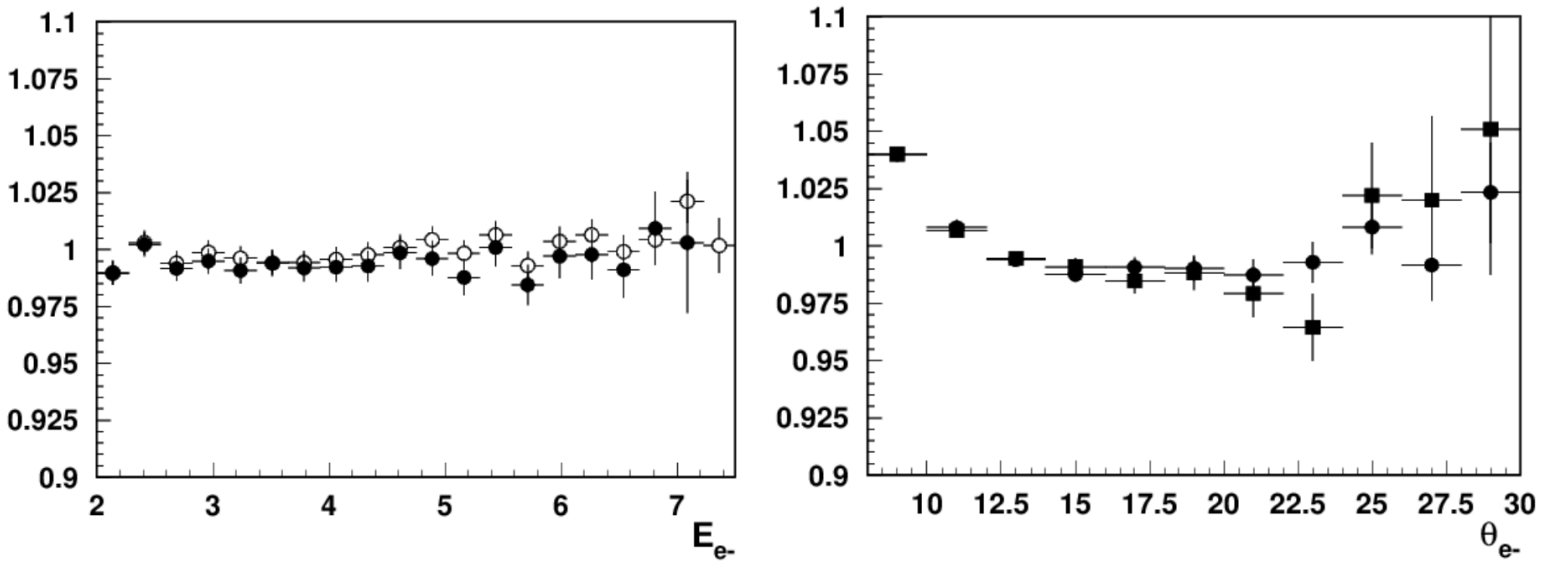

Ratios of normalized counts of electrons for low lumi (5nA) and high lumi (45nA) runs versus the momentum and polar angle of electrons.

Systematic Uncertainties

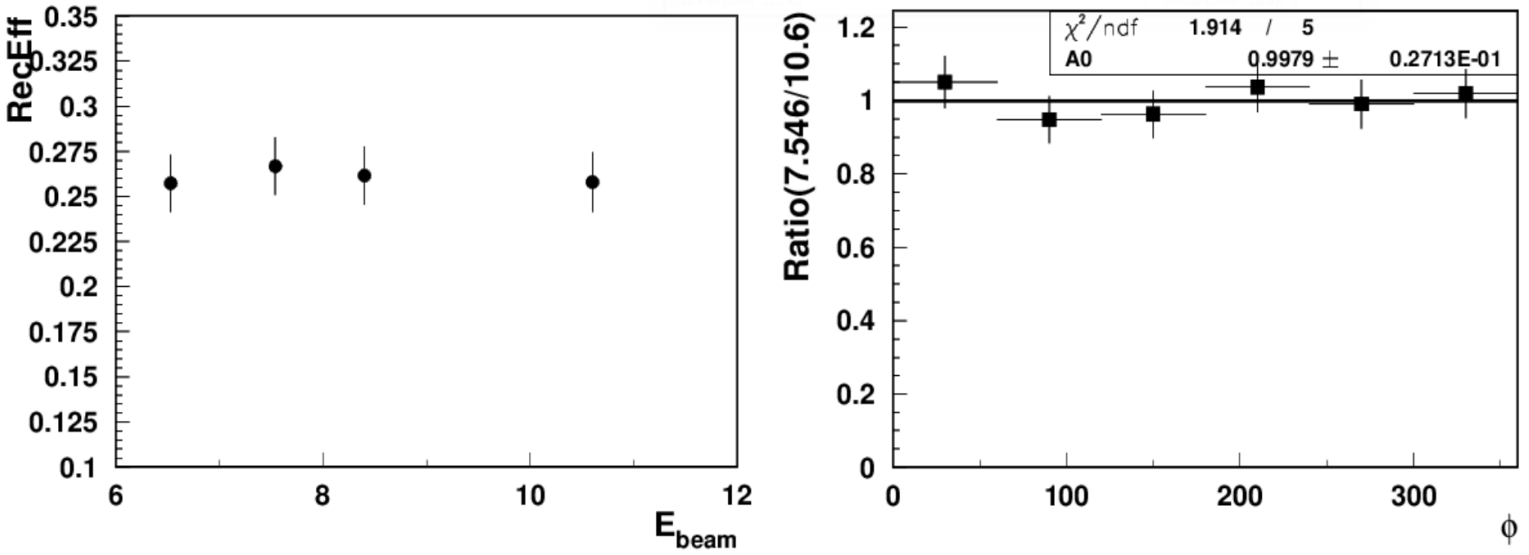

Reconstruction efficiencies from MC (left), and corrected yields from data,
showing normalized to the same counts, dependence on azimuthal angle of electrons (sector dependence).

Inbending Coverage

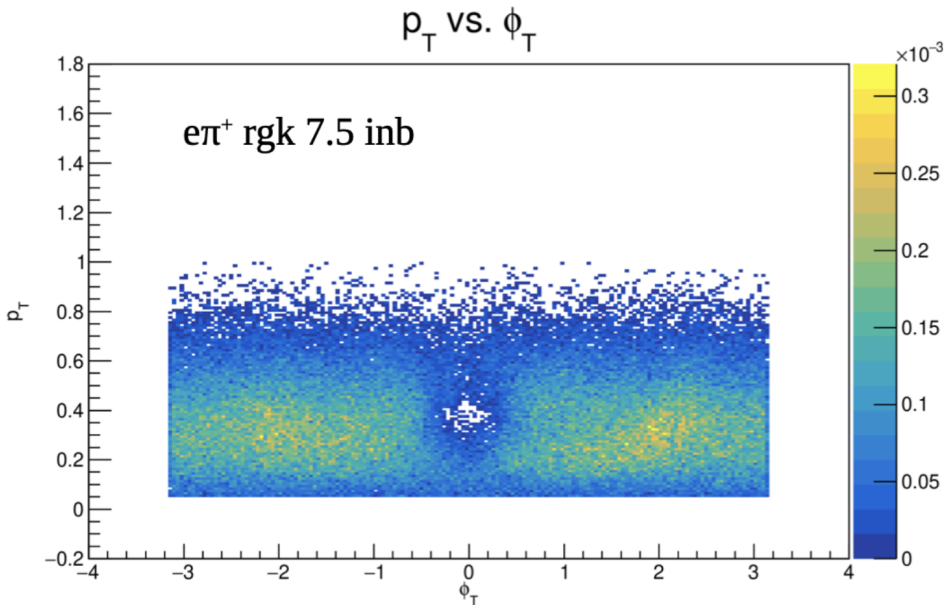

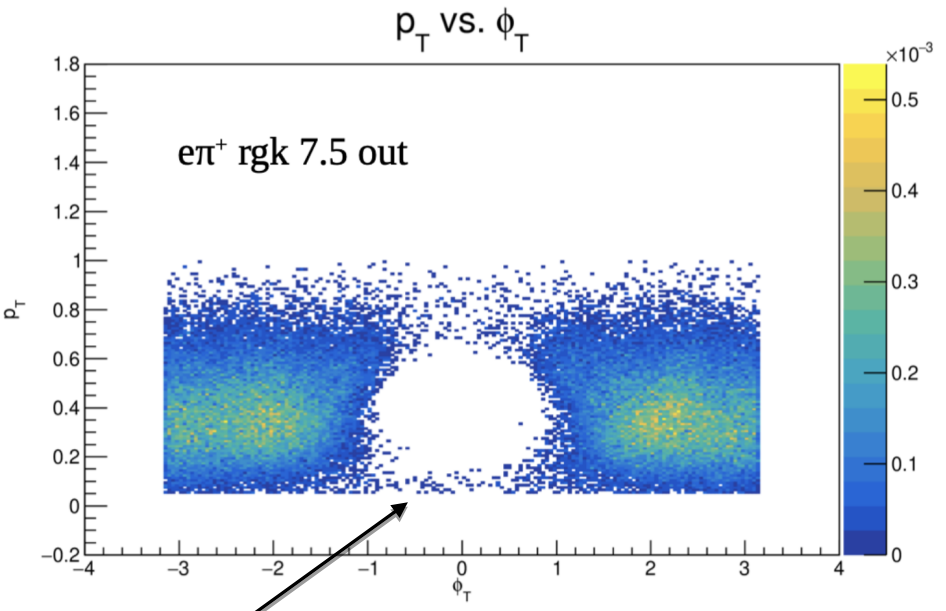

Large gap in coverage for π^+ from -60° to 60° in outbending data

Inbending Coverage

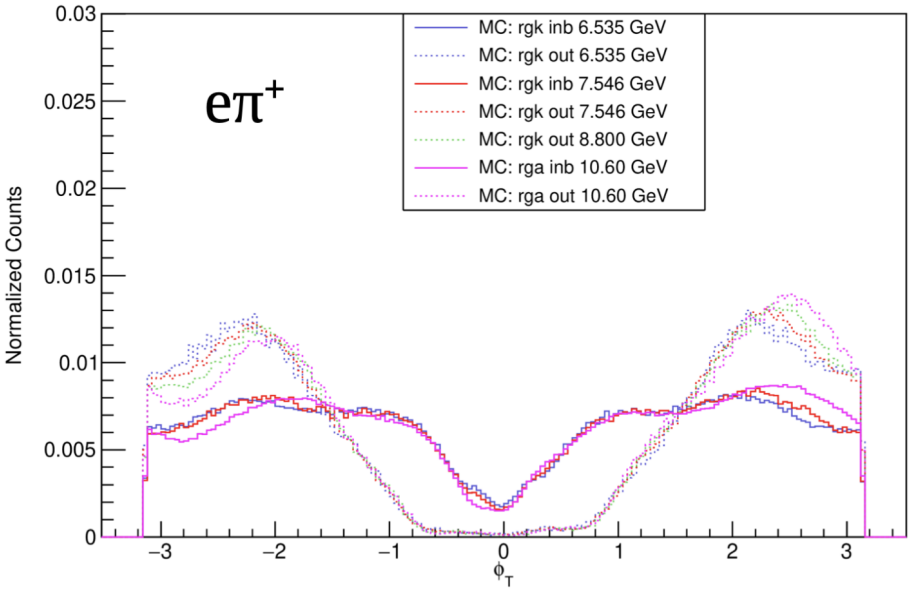

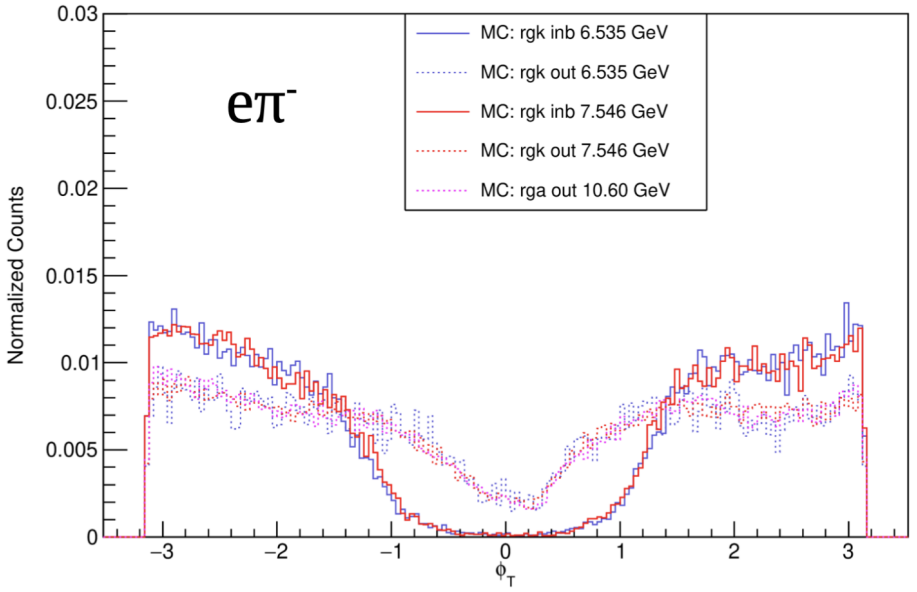

π^- has opposite coverage; π^+ is more interesting first study (and RGA analysis already under way)